J. Math. Biol. (2011) 63:779–799
DOI 10.1007/s00285-010-0387-z

Mathematical Biology

A stability analysis of the power-law steady state of marine size spectra

Samik Datta · Gustav W. Delius · Richard Law · Michael J. Plank

Received: 21 January 2010 / Revised: 2 November 2010 / Published online: 14 December 2010

Abstract This paper investigates the stability of the power-law steady state often observed in marine ecosystems. Three dynamical systems are considered, describing the abundance of organisms as a function of body mass and time: a "jump-growth" equation, a first order approximation which is the widely used McKendrick–von Foerster equation, and a second order approximation which is the McKendrick–von Foerster equation with a diffusion term. All of these yield a power-law steady state. We derive, for the first time, the eigenvalue spectrum for the linearised evolution operator, under certain constraints on the parameters. This provides new knowledge of the stability properties of the power-law steady state. It is shown analytically that the steady state of the McKendrick–von Foerster equation without the diffusion term is always unstable. Furthermore, numerical plots show that eigenvalue spectra of the McKendrick–von Foerster equation with diffusion give a good approximation to those of the jump-growth equation. The steady state is more likely to be stable with a low preferred predator:prey mass ratio, a large diet breadth and a high feeding efficiency. The effects of demographic stochasticity are also investigated and it is concluded that these are likely to be small in real systems.

S. Datta (✉)
Departments of Biology and Mathematics, University of York, Heslington, York YO10 5DD, UK
e-mail: sd550@york.ac.uk

G. W. Delius
Department of Mathematics, University of York, Heslington, York YO10 5DD, UK
e-mail: gwd2@york.ac.uk

R. Law
Department of Biology, University of York, Heslington, York YO10 5DD, UK
e-mail: rl1@york.ac.uk

M. J. Plank
Department of Mathematics and Statistics, University of Canterbury, Christchurch, New Zealand
e-mail: M.Plank@math.canterbury.ac.nz

Mathematics Subject Classification (2000) Primary 92D40; Secondary 92D25

Keywords Marine ecosystem · Stability · Size-spectrum · McKendrick–von Foerster equation · Predator–prey · Growth diffusion · Eigenvalues

1 Introduction

It is well established that marine ecosystems often show roughly equal abundances of biomass in logarithmically increasing weight intervals, when organisms are identified by body mass rather than by species identity (Sheldon et al. 1972; Boudreau and Dickie 1992). This is equivalent to a power-law for the abundance density as a function of body mass with exponent of approximately -2. Alternatively, plotting log(abundance) against log(mass) gives a "size spectrum" (Sheldon and Parsons 1967; Platt and Denman 1978) which is approximately linear with gradient near to -1.

This empirical pattern has motivated a programme of theoretical research. Silvert and Platt (1978, 1980) developed a size-dependent partial differential equation modelling growth and death in a size spectrum, and established the existence of a power-law steady state. The power-law steady state has also been shown in systems where predators are allowed to eat any prey smaller than themselves (Camacho and Solé 2001). When predators are assumed to be more selective (i.e. eating only a certain range of prey), the existence of a power-law steady state has also been proven, using an integro-differential equation for the model instead of a partial differential equation; the exponent generally depends on assimilation efficiency, external mortality and predator–prey interaction rates (Benoît and Rochet 2004). In these and other studies (e.g. Andersen and Beyer 2006; Blanchard et al. 2009; Law et al. 2009), the McKendrick–von Foerster equation is commonly used. However, a derivation from a stochastic model of predation leads to a more general equation (Datta et al. 2010), which we will refer to as the "jump-growth" equation in the following analysis. The McKendrick–von Foerster equation is the first order approximation (in an infinite series) to the jump-growth equation when prey are typically much smaller than predators. The second order approximation brings a diffusion term into the McKendrick–von Foerster equation (Datta et al. 2010), the effects of which have not previously been studied.

Marine biologists need to understand the resilience of the power-law steady state to perturbations caused by fishing and natural phenomena, such as springtime plankton blooms. For instance, it has been shown that fishing increases the temporal variability in abundance of marine species (Hsieh et al. 2006; Anderson et al. 2008). Fundamental to this understanding are the stability properties of the power-law steady state, about which very little is known. We do know from recent numerical studies on the jump-growth equation and the McKendrick–von Foerster equation that there is a bifurcation from a stable power-law steady state to a travelling-wave attractor under certain parameter conditions (Law et al. 2009; Datta et al. 2010). However, the only stability analysis we are aware of assumed growth to be independent of prey density (Arino et al. 2004), thereby excluding a key predator–prey interaction at the heart of the dynamics. The

power-law steady state plays a pivotal role in marine ecosystems, and it is essential to understand the factors that contribute to its stability and instablity.

This paper provides the first detailed stability analysis on the jump-growth equation and its low order approximations, the McKendrick–von Foerster equation and the McKendrick–von Foerster equation with diffusion. It is also the first analysis of the effects of including the second order diffusion term in the McKendrick–von Foerster equation, and of the effects of demographic noise on the stable power-law steady state. The results show that the first order approximation is unstable, whereas the second order approximation can be stable, and gives a much better approximation to the jump-growth equation. The steady state is shown to be more likely to be stable when the preferred predator:prey mass ratio is reduced and the diet breadth and the feeding efficiency are increased.

For readers interested in the mathematical derivation of the perturbation equations and eigenvalue spectra, Sect. 2 shows the necessary steps taken. However, for those more interested in the results of the stability analyses, Sect. 3 shows the behaviour of the three models, and reading Sect. 2.1 should provide sufficient background to understand the different models used.

2 Analysis of the power-law steady state

2.1 Three models of predation

The analysis focuses on perturbations around the power-law steady state of three equations: the jump-growth equation (1), the McKendrick–von Foerster equation (2) and the McKendrick–von Foerster equation with diffusion (3). These equations describe the rate of change in the density of organisms of weight w, which we call $\phi(w)$, with dimensions $\mathrm{M}^{-1}\mathrm{L}^{-3}$, where M is the mass dimension and L is the length dimension. This density is with respect to both mass and volume, so the number of organisms in a volume V with weight between w and $w + dw$ is $V\phi(w)dw$. The first equation is based on the jump-growth equation of Datta et al. (2010),

$$\frac{\partial\phi(w)}{\partial t} = \int \big(-T(w,w')\phi(w)\phi(w') - T(w',w)\phi(w')\phi(w) + T(w - Kw', w')\phi(w - Kw')\phi(w')\big)\, dw' - \mu\phi(w). \tag{1}$$

$T(w, w')$ is proportional to the feeding rate of individuals of weight w on individuals of weight w', and $0 < K < 1$ is the conversion efficiency of biomass from prey to predator (Law et al. 2009). There are three ways in which a feeding event can result in a change in the density of individuals at a given weight w, corresponding to the three terms in the integrand. The first term represents the loss of individuals of weight w due to growth to a larger size (predation of w upon w'), the second term the loss of individuals of weight w due to death (predation of w' upon w), and the third term the gain of individuals of weight w due to growth from from a smaller size (predation of $w - Kw'$ on w'). Here we have also included a linear natural death rate μ (with the dimension of inverse time) to allow for other sources of mortality.

A Taylor expansion of the third term in the jump-growth equation in powers of K gives an infinite series of approximations to the full jump-growth equation (Datta et al. 2010). Expanding up to and including terms linear in K gives our second model, the McKendrick–von Foerster equation,

$$\frac{\partial \phi(w)}{\partial t} = -\int T(w', w)\phi(w)\phi(w')\,dw' - \frac{\partial}{\partial w}\int K w' T(w, w')\phi(w)\phi(w')\,dw' - \mu\phi(w) \tag{2}$$

and including terms quadratic in K gives our third model,

$$\frac{\partial \phi(w)}{\partial t} = -\int T(w', w)\phi(w)\phi(w')\,dw' - \frac{\partial}{\partial w}\int K w' T(w, w')\phi(w)\phi(w')\,dw' + \frac{1}{2}\frac{\partial^2}{\partial w^2}\int (K w')^2 T(w, w')\phi(w)\phi(w')\,dw' - \mu\phi(w), \tag{3}$$

which we will refer to as the McKendrick–von Foerster equation with diffusion. Note that, as in Eq. (1), a linear death rate μ has been included in these two approximations.

We assume a feeding kernel of the form

$$T(w, w') = A w^{\alpha} s\left(\frac{w}{w'}\right) \tag{4}$$

where A is the predator search volume per unit mass$^{-\alpha}$ per unit time, α is the predator search exponent, calculated to have a value of approximately 0.8 (see Ware 1978), and $s(w/w')$ is the feeding preference function, centred around some preferred predator:prey mass ratio B. To make analytical progress in this paper we assume that $\alpha = \gamma - 1$, where γ is the exponent of the power-law steady state (≈ 2). This assumption then has the consequence that the steady state is a power-law (see below). In addition, the eigenvalue spectrum can then be written as a closed form expression and its properties analysed. Although probably not realistic from a biological point of view (discussed in Sect. 4), the assumption places stability analyses of size spectra on a firm mathematical foundation and provides a basis from which exploration of a broader class of systems can begin.

Section 2.2 defines the power-law steady state for the jump-growth equation (1) and its two approximations (2) and (3). Section 2.3 develops equations for the dynamics of small perturbations to this steady state and Sect. 2.4 gives explicit equations for the eigenvalue spectra. In Sect. 2.5, the effect of demographic noise on the system at steady state is investigated. Finally, Sect. 2.6 incorporates a Gaussian feeding preference for predators.

2.2 The power law steady state

The steady state for Eqs. (1), (2) and (3) is given by

$$\hat{\phi}(w) = \phi_0 w^{-\gamma} \tag{5}$$

where ϕ_0 is a constant. Below, it helps to transform the variable w to a dimensionless log weight variable $x = \ln(w/w_0)$ (for some arbitrary weight w_0). For analysing the steady state of the jump-growth equation (1) it is convenient to change the integration variable of each of the three terms to the predator:prey mass ratio, which leads to the transformed equation

$$\begin{aligned}\frac{\partial v(x)}{\partial t} = \hat{A} \int s(e^r)(-e^{\alpha r} v(x) v(x-r) - v(x) v(x+r) \\ + e^{\alpha(r+\psi(r))} v(x-\psi(r)) v(x-r-\psi(r)))\, dr - \mu v(x),\end{aligned} \tag{6}$$

where we have used Eq. (4) for the feeding kernel with $\alpha = \gamma - 1$. Here $v(x)$ has the property that $e^{-(\alpha+1)x} v(x)\, dx = \phi(w)\, dw$ and has dimensions L^{-3}, $\hat{A} = A {w_0}^{\alpha}$, and r is the log of the predator:prey mass ratio with $\psi(r) = \ln(1 + K e^{-r})$. In the transformed jump-growth equation (6), the steady state is simply given by

$$v(x) = v_0, \tag{7}$$

where $v_0 = \phi_0 {w_0}^{-\alpha}$ is a constant. Substituting this into Eq. (6) we get the steady state condition,

$$\int s(e^r) \left(-e^{\alpha r} - 1 + e^{\alpha(r+\psi(r))}\right) dr - \eta = 0 \tag{8}$$

where $\eta = \mu/(\hat{A} v_0)$ is dimensionless. This equation implicitly determines the value of the search volume exponent α (and thus the steady state exponent γ) for a given choice of the parameters K and η and the feeding kernel $s(e^r)$. If we impose the conditions that predators can only feed upon prey smaller than themselves and $K \neq 0$, we can prove analytically that there always exists a unique value for α that solves the steady state condition. Without these conditions we verify its existence and uniqueness numerically. Setting η determines the abundance of fish at the steady state, as it contains the constant v_0.

For the McKendrick–von Foerster equation with diffusion (3), the steady state condition is

$$\int s(e^r) \left(-1 + \alpha K e^{(\alpha-1)r} + \alpha(\alpha-1)\frac{K^2}{2} e^{(\alpha-2)r}\right) dr - \eta = 0, \tag{9}$$

and for the McKendrick–von Foerster equation without diffusion (2), terms of order K^2 in Eq. (9) are ignored.

2.3 Perturbations around the steady state of the jump-growth equation

We now add a small perturbation to the steady state of the jump-growth equation and observe its evolution over time. If the perturbation grows over time, then the steady state is not stable, and the system will not stay at the equilibrium; if the perturbation decays, then the steady state is locally asymptotically stable. We call the perturbation $v_0\epsilon(x,t)$ and obtain its evolution equation by substituting

$$v(x,t) = v_0(1+\epsilon(x,t)) \tag{10}$$

into Eq. (6). We now assume that we can neglect terms of order ϵ^2 because ϵ is taken to be very small. For a finite-dimensional dynamical system this can be justified rigorously using the Hartman–Grobman theorem (see e.g. Kirchgraber and Palmer 1990). However in an infinite-dimensional system this can be more subtle (see e.g. Aulbach and Garay 1993) and we proceed formally in analogy with the finite-dimensional case. We then use condition (8) to eliminate terms of order ϵ^0, so that only terms of ϵ^1 remain. This leads to the linearised perturbation equation

$$\begin{aligned}\frac{\partial\epsilon(x)}{\partial t} = \hat{A}v_0 \int s(e^r)\Big(&- e^{\alpha r}(\epsilon(x)+\epsilon(x-r)) - (\epsilon(x)+\epsilon(x+r)) \\ &+ e^{\alpha(r+\psi(r))}(\epsilon(x-\psi(r))+\epsilon(x-r-\psi(r)))\Big)\,dr - \mu\epsilon(x).\end{aligned} \tag{11}$$

We can change integration variables appropriately so that the right hand side of equation (11) is in the form of an integral operator acting on ϵ,

$$\frac{\partial\epsilon(x)}{\partial t} = \hat{A}v_0 \int \epsilon(m)G(x,m)\,dm \tag{12}$$

where

$$\begin{aligned}G(x,m) = -\delta(r)\left(\int s(e^z)(e^{\alpha z}+1)\,dz + \mu\right) - s(e^r)e^{\alpha r} - s(e^{-r}) \\ + s(e^{z_1})K^{-1}e^{(\alpha+1)(z_1+r)} + s(e^{z_2})e^{(\alpha+1)r-z_2}.\end{aligned} \tag{13}$$

Here $r = x-m$, $z_1 = \ln(K/(e^r-1))$, $z_2 = \ln(e^r-K)$ and δ represents the Dirac delta function. The integral kernel $G(x,m)$ can be thought of as an infinite-dimensional version of a matrix with indices x and m and the task of solving Eq. (12) thus reduces to finding the 'eigenvectors' and 'eigenvalues' of this 'matrix'. To define the operator rigorously in the infinite-dimensional case we must first restrict the perturbations to the space of square-integrable periodic functions with some period L. On this space the operator is compact and thus it is meaningful to speak of its spectrum of eigenvalues. In the end we can then take the period L to infinity.

2.4 Eigenvalue spectra

We observe that the integral kernel $G(x, m)$ depends on $x - m$ only, i.e. it is a convolution kernel. Its 'eigenvectors' are given by plane waves, $\epsilon_k(x) = e^{ikx}$, for any $k \in \mathbb{R}$. We refer to k as the wavenumber of the plane wave $\epsilon_k(x)$ and denote the corresponding eigenvalue as $\lambda(k)$.

The eigenvalues are

$$\lambda(k) = \int s(e^r) \left(-e^{\alpha r} - e^{ikr} + e^{\alpha r + (\alpha - ik)\psi(r)}\right)\left(1 + e^{-ikr}\right) dr - \eta. \tag{14}$$

We refer to the values taken by $\lambda(k)$ as the eigenvalue spectrum.

A general perturbation can then be expanded in terms of these plane waves and its time evolution is

$$\epsilon(x, t) = \int C(k) e^{ikx + \hat{A} v_0 \lambda(k) t}\, dk. \tag{15}$$

The expansion coefficient function $C(k)$ is an even function because $\epsilon(x, t)$ is real. Notice that if any $\lambda(k)$ has a positive real part then perturbations grow exponentially with time (the factors $\hat{A}$ and v_0 are positive constants and thus do not affect the coefficient of t), which means that the steady state is unstable.

To derive the eigenvalue spectrum for the McKendrick–von Foerster equation with diffusion from Eq. (14), $\psi(r)$ is expanded in powers of K. Taking terms up to and including K^2 yields

$$\lambda(k) = \int s(e^r) \left(-e^{ikr} + K(\alpha - ik)e^{(\alpha-1)r} + \frac{K^2}{2}(\alpha - ik)(\alpha - 1 - ik)e^{(\alpha-2)r}\right) \times \left(1 + e^{-ikr}\right) dr - \eta. \tag{16}$$

As in Eq. (9), neglecting K^2 terms gives the corresponding eigenvalue spectrum for the McKendrick–von Foerster equation.

It is the real part of the eigenvalue that we are interested in, as it is the sign of this that determines whether the perturbations grow or die out over time. If, for some wavenumber k $\mathrm{Re}(\lambda(k))$ is positive, then any perturbation containing a component with this wavenumber will grow over time and thus the steady state will be unstable. If $\mathrm{Re}(\lambda(k))$ is negative for all k then all perturbations die out over time, and the steady state is stable.

2.5 Stochastic fluctuations

The analysis above is concerned with the deterministic jump-growth equation (1) and its low-order approximations (2) and (3). In fact, Eq. (1) is the mean-field equation for a stochastic model of pairwise encounters between predator and prey (Datta et al.

2010). The magnitude of the fluctuations due to the demographic noise in the stochastic model is usually a factor of $\Omega^{\frac{1}{2}}$ smaller than the mean-field solution, where Ω is the number of individuals in the system (van Kampen 1992). For marine ecosystems Ω tends to be very large, so the fluctuations will be relatively small, but they can nonetheless have important effects (McKane and Newman 2005), and may significantly impact the patterns observed in empirical data.

In this section we describe how the magnitude of the stochastic fluctuations, and the correlations between the fluctuations at different body sizes, can be predicted. In order to make the following statements rigorous, one would work in terms of discrete body size intervals, but we work in the continuum formally for convenience, which gives the same results. We let $n(x,t)$ be a random variable corresponding to the density of individuals of size $w = w_0 e^x$ at time t. The random variable is described by the stochastic process given in previous work (Datta et al. 2010). Following the method used by van Kampen (1992), we separate $n(x,t)$ into a deterministic component $v(x,t)$, which satisfies the mean-field equations studied above, and a random fluctuation component $\xi(x,t)$:

$$n(x,t) = Ve^{-\alpha x}\left(v(x,t) + \Omega^{-\frac{1}{2}} v_0 \xi(x,t)\right). \tag{17}$$

Since the focus of this paper is the stability of the steady state, we restrict attention to the case where the deterministic component is at steady state; the results are therefore only relevant in cases where the steady state is stable. The stochastic fluctuations $\xi(x,t)$ can be described by a Langevin-type equation

$$\frac{\partial}{\partial t}\xi(x,t) = \hat{A}v_0\left(\int G(x,y)\xi(y,t)dy + \rho(x,t)\right), \tag{18}$$

where the kernel G is given by Eq. (13) and $\rho(x,t)$ is a null-mean noise process. Details of the derivation of this equation in the general, non-equilibrium setting may be found in Datta et al. (2010). The covariance of noise at two different body sizes is described by a covariance kernel $B(x,y) = \langle \rho(x,t)\rho(y,t)\rangle$, which is given by (see Datta et al. 2010):

$$\begin{aligned} B(x,y) = e^{\alpha(x+y)} \int \Bigg(& f(x,y,z) - f(x,z,y) - f(z,y,x) \\ & + \delta(x-y) \int \left(f(x,z,z') + \frac{f(z,z',x)}{2} \right) dz' \Bigg) dz, \end{aligned} \tag{19}$$

where

$$f(x,y,z) = e^{-\alpha(x+y)}\left(k(x,y,z) + k(y,x,z)\right) \tag{20}$$

and

$$k(x,y,z) = e^{\alpha x} s\left(e^{x-y}\right)\delta(z - x - \psi(x-y)). \tag{21}$$

The covariance $\langle \xi(x,t)\xi(y,t)\rangle$ of the fluctuations at logarithmic body sizes x and y satisfies

$$\frac{\partial}{\partial t}\langle \xi(x,t)\xi(y,t)\rangle = \hat{A}v_0 \left(\int \left(G(x,z)\langle \xi(z,t)\xi(y,t)\rangle + G(y,z)\langle \xi(z,t)\xi(x,t)\rangle \right) dz + B(x,y) \right). \tag{22}$$

In the steady state, the time derivative on the left-hand side vanishes and thus the covariance function $\langle \xi(x,t)\xi(y,t)\rangle$ can be calculated by setting the right-hand side to zero which results in a linear equation to be solved. We present the numerical results of this in Sect. 3.7. In order to verify these, we also carry out stochastic simulations of the number $n_i(t)$ of individuals in log weight bracket $[x_i, x_{i+1}]$ for $-4 \le x \le 4$ (outside this size range, the spectrum is assumed to remain at steady state). We approximate the number R_{ij} of individuals in bracket i that eat an individual in bracket j during a short time δt as a Poisson random variable (see Datta et al. 2010, for details). The mean of R_{ij} is given by

$$V^{-1}T(w_0 e^{x_i}, w_0 e^{x_j}) n_i(t) n_j(t) \delta t. \tag{23}$$

The fluctuation $\xi(x_i,t)$ is computed from the difference between $n_i(t)$ and its equilibrium value. The covariance $\langle \xi(x_i,t)\xi(x_j,t)\rangle$ is then obtained by averaging $\xi(x_i,t)\xi(x_j,t)$ over a large number of successive time points. In the long term, this gives the same result as the ensemble average of $\xi(x_i,t)\xi(x_j,t)$ provided the stochastic process is ergodic.

2.6 Gaussian feeding preference

Organisms do not eat indiscriminately; here we assume that they feed at some preferred prey size (in relation to their own size), and a range of sizes around this preferred size. To reflect this, a suitable preference function is a Gaussian feeding preference, with peak at β and width proportional to σ (Andersen and Beyer 2006; Law et al. 2009). This can be represented by the following form for $s(e^r)$,

$$s(e^r) = \frac{1}{\sqrt{2\pi}\sigma} \cdot e^{\frac{-(r-\beta)^2}{2\sigma^2}}. \tag{24}$$

In theory this function allows predators to eat prey larger than themselves (i.e. is non-zero for $r < 0$), although for realistic sets of parameter values $s(e^r)$ is typically negligible for $r < 0$.

The eigenvalue spectrum for the jump-growth equation (14) with the Gaussian preference function (24) unfortunately does not have a closed form. In contrast, the eigenvalue spectra for the McKendrick–von Foerster equation without and with diffusion

can be determined analytically. Defining

$$R_n = (\alpha - n)\left(\beta + \frac{1}{2}\sigma^2(\alpha - n)\right) \tag{25}$$

$$I_n = k(\beta + \sigma^2(\alpha - n)), \tag{26}$$

and taking the steady state condition (9) into account, the eigenvalue spectrum for the equation with diffusion gives

$$\begin{aligned}\mathrm{Re}(\lambda(k)) = e^{-\frac{1}{2}\sigma^2 k^2}\Bigg[&- \cos(k\beta) + Ke^{R_1}(\alpha\cos(I_1) - k\sin(I_1)) \\ &+ \frac{K^2}{2}e^{R_2}((\alpha(\alpha-1) - k^2)\cos(I_2) - k(2\alpha - 1)\sin(I_2))\Bigg] \\ &- \frac{K^2}{2}e^{R_2}k^2. \end{aligned} \tag{27}$$

The diffusion term is removed by excluding terms of order K^2 in Eq. (27). An important difference between the two approximations is that there must always exist values of k for which $\mathrm{Re}(\lambda(k))$ is positive in the eigenvalue function for the McKendrick–von Foerster equation. Consequentially the McKendrick–von Foerster equation will never give a stable spectrum. In contrast, the McKendrick–von Foerster equation with diffusion contains a non-oscillatory term in k which is negative and increases in magnitude as k increases. This has the effect of making the real parts of the eigenvalues more negative for higher values of k. For both approximations the oscillatory terms are damped by a factor of $e^{-\frac{1}{2}\sigma^2 k^2}$. Equation (27) is analysed in greater detail in Sect. 3 to explain observed patterns in the behaviour of eigenvalue spectra when altering parameters.

Using the steady state condition (8), it can be shown for the jump-growth equation that $\mathrm{Re}(\lambda(0)) = \eta$. This result also applies to both of the approximations. Thus, for any positive η, $\mathrm{Re}(\lambda(k))$ must be positive at $k = 0$, and as $\lambda(k)$ given in Eq. (14) is continuous, there exists a neighbourhood around $k = 0$ where $\mathrm{Re}(\lambda(k)) > 0$. Therefore there will be a range of wavenumbers k for which perturbations e^{ikx} will destabilise the steady state. However, we only expect our model to be realistic for a range of body weights spanning around 12 orders of magnitude (Cohen et al. 2003) and therefore should ignore perturbations with a wavelength longer than this, i.e. those with wavenumbers smaller than about $k \approx 0.2$.

3 Results

3.1 Eigenvalue spectra of the three models

To evaluate the eigenvalue spectra, we use the Gaussian feeding preference (24), for given values for the parameters K, β, σ, η. Where possible we keep these parameters

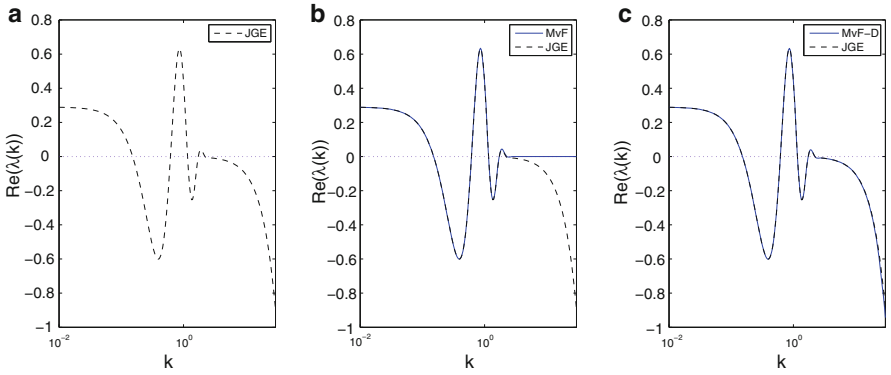

Fig. 1 The eigenvalue spectra for the **a** jump-growth equation (JGE), **b** McKendrick–von Foerster equation (MvF) and **c** McKendrick–von Foerster equation with diffusion (MvF-D) when using a Gaussian feeding preference. Note that η has been set to give a steady state exponent of roughly 2.3 for all three spectra. Parameter values $K = 0.2,\ \beta = 5,\ \sigma = 1.5,\ \eta = 0.290, \gamma = 2.30$

biologically reasonable and close to values from previous studies (Andersen and Beyer 2006). We use values of K=0.2, β=5 and σ=1.5 as a base parameter set, and investigate the effects of changing these parameters. For this base parameter set, the steady state exponent γ is equal to 2.27 when η=0 (i.e. no external mortality) and the value of γ increases with η. The values of γ used in the numerical plots mostly lie in the empirical range of 2.2–3.25 reported by Blanchard et al. (2009). Values of the wavenumber k are taken over a range from 0 to 30, as the interesting behaviour of the eigenvalue spectra is seen in this frequency range. Note that the expressions for $\mathrm{Re}(\lambda(k))$ are even in k for the three models, so the plotting of negative values of k is unnecessary. We often plot the eigenvalue spectra over a logarithmic k-axis to make it easier to see the details at small k.

Examples of the eigenvalue spectra of the jump-growth equation and its two approximations (all computed numerically using the preference function (24)) are compared in Fig. 1. All three spectra are close to η for small k, as expected from Sect. 2.6. Both approximations are close to the jump-growth equation for low values of k, but as k gets larger only the McKendrick–von Foerster equation with diffusion follows the jump-growth equation closely. This is expected from Eq. (27) because the diffusion term is needed to make the eigenvalue spectrum more negative with increasing k. Adding the diffusion term gives a better approximation to the full jump-growth model. Thus the properties of Eq. (27) will be used to gain insight into the behaviour of the eigenvalue spectra of the jump-growth equation in the subsequent sections.

The power-law steady state is unstable for all three models in this example, because all three spectra contain eigenvalues with a positive real part (the maximum occurring at $k \approx 0.861$). The tendency for unstable steady states to emerge in our analysis will be discussed in Sect. 4.

The different behaviours of the two approximations are not just limited to a Gaussian feeding preference; similar results have also been obtained when using a step function for the feeding preference (results not shown here). This has the form

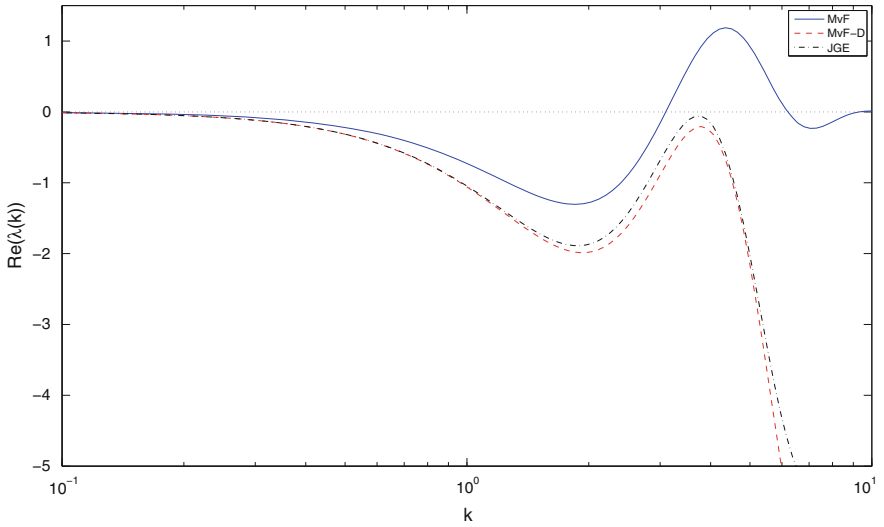

Fig. 2 Eigenvalue spectra for the McKendrick–von Foerster equation and McKendrick–von Foerster equation with diffusion, compared to that of the jump-growth equation. Parameter values $K = 0.8$, $\beta = 1$, $\sigma = 0.35$, $\eta = 0$, $\gamma = 2.11$

$$s(e^r) = \begin{cases} \frac{1}{2\sigma} & \text{if } \beta - \sigma \leq r \leq \beta + \sigma \\ 0 & \text{otherwise} \end{cases} \tag{28}$$

and is a rectangular shaped function, with midpoint β, width 2σ and height $1/(2\sigma)$. It is worth noting that although behaviour similar to Fig. 1 is observed, the oscillations are not damped exponentially, and oscillations are observed at all values of k.

3.2 Stable and unstable steady states

For some sets of parameter values, the steady state is stable. Figure 2 gives an example, obtained by allowing a low preferred predator:prey mass ratio β, a high efficiency K and a relatively large diet breadth σ. This example is chosen to illustrate the point that the eigenvalue spectrum for the McKendrick–von Foerster equation can be misleading; the spectrum for the McKendrick–von Foerster equation without diffusion peaks at 1.19, whereas for the equation with diffusion and the jump-growth equation $\mathrm{Re}(\lambda(k)) < 0$ for all k. The spectrum is stabilised by the non-oscillatory term introduced by the inclusion of terms of order K^2. The diffusion term contributes to stability and the effect of this is great enough to make a qualitative difference to the calculated stability of the steady state. As predicted in Sect. 2.6, the McKendrick–von Foerster equation gives an unstable spectrum for any choice of parameter values.

3.3 Time evolution of perturbations

To show the consequences of stable and unstable steady states on the dynamics, we can examine the behaviour of a local perturbation to the size spectrum, and observe its time evolution. Assume a Gaussian perturbation with initial form

$$\epsilon(x,0) = \nu e^{-\frac{x^2}{2\varsigma^2}}, \tag{29}$$

where ν is a small constant and ς dictates what range of body sizes in the size spectrum are effected by the initial perturbation. This can be expanded in plane waves, rewriting $\epsilon(x,0)$ as

$$\epsilon(x,0) = \bar{\nu} \int_{-\infty}^{\infty} e^{-\frac{1}{2}\varsigma^2 k^2} e^{ikx}\, dk. \tag{30}$$

where $\bar{\nu} = (\nu\varsigma)/\sqrt{2\pi}$. The time dependence of this perturbation then has the following form:

$$\epsilon(x,t) = \bar{\nu} \int_{-\infty}^{\infty} e^{-\frac{1}{2}\varsigma^2 k^2} e^{ikx + \hat{A}v_0\lambda(k)t}\, dk. \tag{31}$$

We set ς so that the perturbation covers about one size unit on the x-scale, and choose units so that $\hat{A}v_0 = 1$. We choose to centre our perturbation around $x = 0$ without loss of generality. Plotting the time evolution both for a stable spectrum (Fig. 2) and an unstable spectrum (Fig. 1) using the jump-growth equation gives the two behaviours shown in Fig. 3.

For both plots, the initial perturbation moves along the x-axis over time, as the organisms it contains feed on smaller organisms and grow. In the case of a stable spectrum, the perturbation gives rise to smaller peaks either side of the initial perturbation, and these all die out over time, tending to zero across the whole range of x. In the case of an unstable spectrum, the peaks grow over time. They develop into waves with wavenumber $\hat{k}$, where $\hat{k}$ is the most unstable node of the eigenvalue spectrum. Thus, in the case of Fig. 3b, where $\hat{k} = 0.861$, the wavelength of the peaks is seen to be around $(2\pi)/\hat{k}$. Over time the peaks grow in magnitude but maintain their wavelength. The speed at which the perturbation moves through the size spectrum is determined by $\mathrm{Im}(\lambda(\hat{k}))$.

3.4 Changing the preferred predator : prey mass ratio

Figure 4 shows the effect of increasing the logarithm of the preferred predator:prey mass ratio β on the stability of the jump-growth equation. The maximum real part of the eigenvalues increases as β increases, the steady state going from stability when

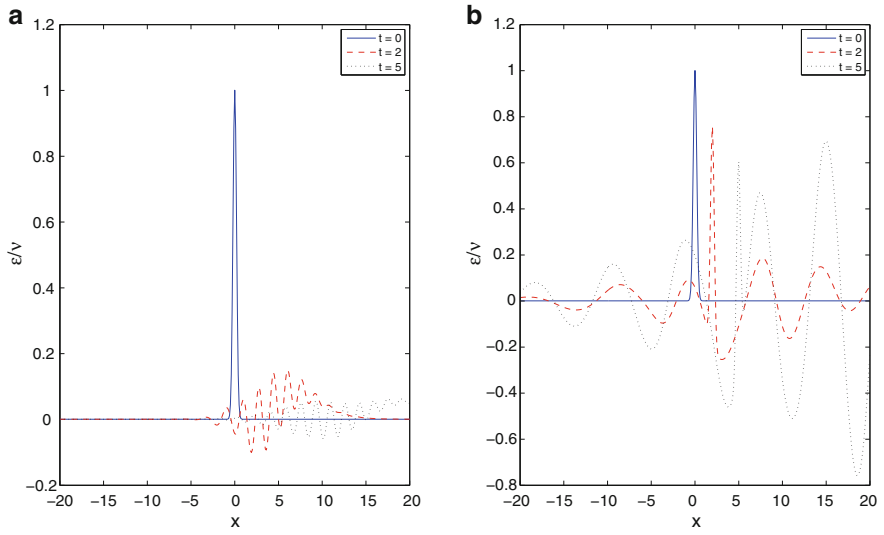

Fig. 3 The time evolution of a Gaussian perturbation when using the jump-growth equation, $\varsigma = 0.2$, when using **a** a stable eigenvalue spectrum (parameter values $K = 0.8,\ \beta = 1,\ \sigma = 0.35,\ \eta = 0, \gamma = 2.11$), and **b** an unstable eigenvalue spectrum (parameter values $K = 0.2,\ \beta = 5,\ \sigma = 1.5,\ \eta = 0.290, \gamma = 2.30$)

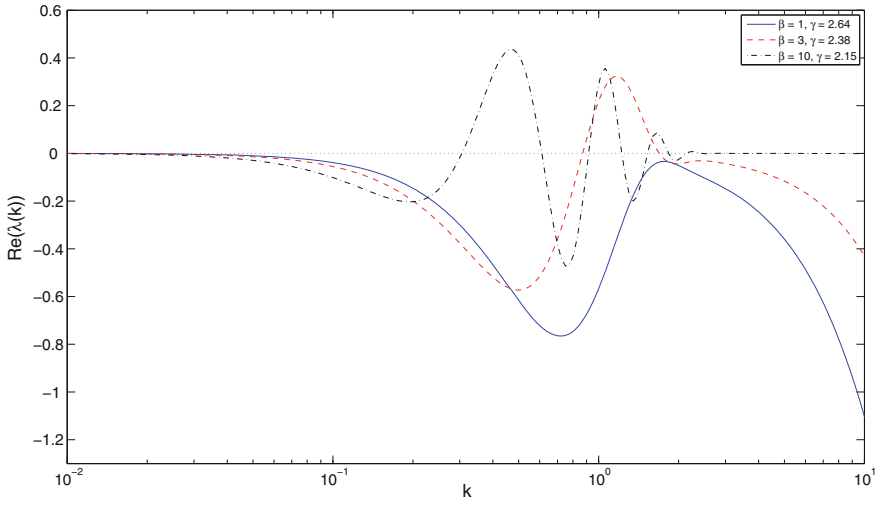

Fig. 4 The eigenvalue equations for the jump-growth equation with varying logarithm of the preferred predator : prey mass ratio β. Parameter values $\sigma = 1.5,\ K = 0.2,\ \eta = 0$

$\beta = 1$ (i.e. $\mathrm{Re}(\lambda(k)) < 0$ for all k), to instability for the larger values of β. This is in keeping with previous numerical results, where increasing β led to a bifurcation from the power-law steady state to a travelling wave attractor (Law et al. 2009), although the two results should not be directly compared because in earlier work the assumption $\alpha = \gamma - 1$ was not imposed. The changes seen in Fig. 4 as β is increased can be

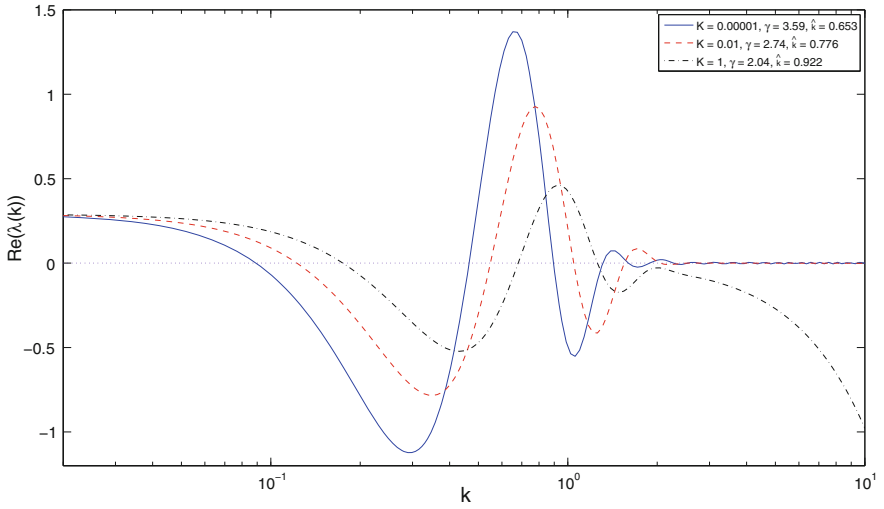

Fig. 5 The eigenvalue equations for the jump-growth equation, with varying feeding efficiency K; $\hat{k}$ denotes the location of the most unstable node of the spectrum. Parameter values $\beta = 5,\ \sigma = 1.5, \eta = 0.290$

understood in terms of Eq. (27), where β occurs both in the R_n exponential terms and in the I_n cosine and sine terms. In R_n, β acts to dampen the waves more as it increases, and in I_n, β acts to reduce the period of the waves as it increases. Both these changes are visible in the figure. Some decrease in the exponent of the power-law steady state is also evident with increasing β in Fig. 4. We interpret this in biological terms as an outcome of less biomass being lost from the size spectrum as β increases, because biomass is inefficiently consumed fewer times during its passage along the spectrum. Note that σ has been held constant this figure, so that as β is increased, the mean of the predator:prey feeding distribution increases but the variance remains constant.

3.5 Changing the feeding efficiency

Figure 5 shows the effect of changing the feeding efficiency K on the eigenvalue spectrum. To understand Fig. 5, it helps to consider the limiting case of $K \to 0$. Although unrealistic, because it implies no growth of organisms, the eigenvalue spectrum in Eq. (27) is then simply a damped cosine wave: $\mathrm{Re}(\lambda(k)) = e^{-\frac{1}{2}\sigma^2 k^2} \cos(k\beta)$. Consequently, the most unstable node $\hat{k}$ must be the first peak of this wave, which occurs at $\hat{k} = \pi/\beta$, equivalent to $\hat{k} = 0.628$ with the parameter values in Fig. 5. We observe in Fig. 5 that, for small K (1×10^{-5}), the value of $\hat{k}$ (0.655) is close to this limiting value.

Corresponding to the node at $\hat{k} = \pi/\beta$, there is a dominant eigenfunction with a wavelength 2β. This can be understood in biological terms as a straightforward consequence of the predator–prey interaction. A pulse perturbation from steady state that increases the density of predators at some size lowers the density of prey e^{β} times smaller than themselves. This in turn reduces the mortality rate on the prey's prey $e^{2\beta}$

times smaller than the predators, allowing their density to increase. This leads to the wavelength 2β.

Figure 5 also shows that, as K increases, $\hat{k}$ grows and $\mathrm{Re}(\lambda(\hat{k}))$ gets smaller. In other words, as K increases, perturbations from the steady state have wavelengths progressively less than 2β and grow more slowly. In this case, a pulse increase in predator density at some body size does not remain at the same position in the size spectrum as time goes on. The predators grow as they eat, and their preferred prey body size moves along with them. This mitigates to some extent the destabilizing feedback of slow (or absent) predator growth that would continue to reduce the density of prey approximately e^{β} times smaller than the predator. These results help explain the observation of Law et al. (2009) that perturbations tend to have a wavelength less than 2β. Notice also that the exponent of the power-law steady state becomes substantially smaller as K increases, because more biomass passes along the size spectrum to large organisms.

3.6 Changing diet breadth

It has been shown in earlier numerical studies that, by making the diet breadth more narrow (i.e. decreasing σ), the power-law steady state can become unstable, leading to travelling waves of abundance that move along the spectrum with time (Law et al. 2009; Datta et al. 2010). In the extreme case of a feeding kernel where predators only eat prey of the exact preferred mass ratio, and of no other weight (using a Dirac delta function of the form $s(e^r) = \delta(r - \beta)$ as the feeding preference), the steady state can be shown always to be unstable (proof not given here).

In Fig. 6 we investigate the effect of increasing the diet breath σ. As σ increases, the amplitude of oscillations at low values of k decreases, and the range for which $\mathrm{Re}(\lambda(k))$ has positive values becomes narrower; the largest value of k for which $\mathrm{Re}(\lambda(k)) > 0$ k^* is seen to decrease as σ increases. This is consistent with Eq. (27), because increasing σ will cause the oscillations to be damped sooner by the $e^{-\frac{1}{2}\sigma^2 k^2}$ term. Note that it is the change in σ which is causing the change in the spectrum and not the steady state exponent; γ remains at a value of approximately 2.27 in each case.

3.7 The effects of demographic stochasticity

As explained in Sect. 2.5, we can calculate the equal-time covariance function $\langle \xi(x,t)\xi(y,t)\rangle$ for the fluctuations in the steady state. This function describes how the fluctuations due to demographic stochasticity are correlated at different weights at steady state. It is obtained by solving the linear integral equation obtained by setting the time derivative to zero in Eq. (22). To perform the calculation we use discrete weight brackets, so that the integral equation becomes a matrix equation, which we solve numerically.

Using the same parameter values as in Fig. 2, the covariance function calculated from (22) (solid curve) and from stochastic simulations (points) is plotted in Fig. 7. The simulations use a system size of $\Omega = 10^5$ and are restricted to the size range $-4 \le x \le 4$; simulating a wider size range for sufficient time would be computationally

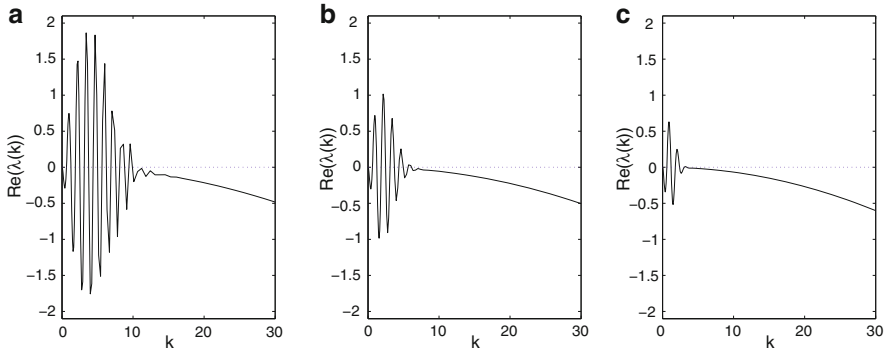

Fig. 6 The eigenvalue spectra for the jump-growth equation with varying diet breadth: **a** $\sigma = 0.25$ ($k^* = 9.60$), **b** $\sigma = 0.5$ ($k^* = 6.02$), and **c** $\sigma = 1$ ($k^* = 3.41$), where k^* denotes the largest value of k for which $\mathrm{Re}(\lambda(k)) > 0$. Parameter values $K = 0.2,\ \beta = 5,\ \eta = 0,\ \gamma = 2.27$

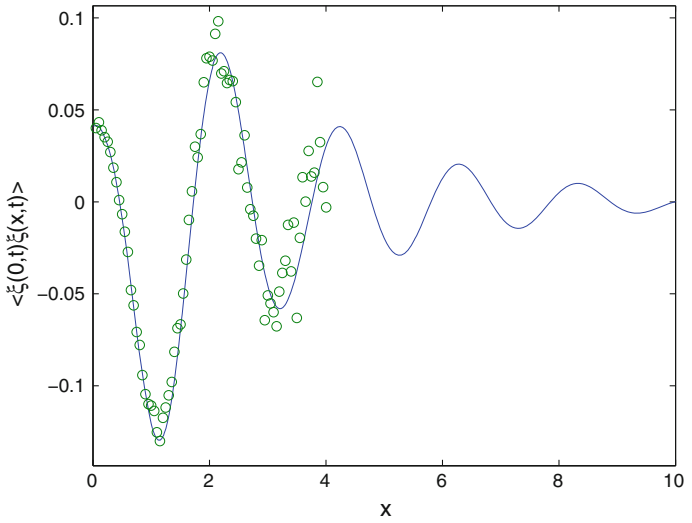

Fig. 7 The covariance function $\langle \xi(0,t)\xi(x,t)\rangle$ for the fluctuations around a stable steady state due to demographic stochasticity (*solid curve* solution of Eq. (22); *points* stochastic simulations). This measures the covariance between stochastic fluctuations at log body sizes 0 and x; the covariance between fluctuations at log body sizes x and y, $\langle \xi(x,t)\xi(y,t)\rangle$, is equal to $e^{\alpha x}\langle \xi(0,t)\xi(y-x,t)\rangle$. Parameter values $K = 0.8,\ \beta = 1,\ \sigma = 0.35,\ \eta = 0, \gamma = 2.11$

prohibitive. The simulation data become increasingly noisy as x increases, due to the decreasing number of individuals in a weight bracket. Nevertheless, the simulation results show good agreement with the solution of Eq. (22).

The graph in Fig. 7 decays exponentially with distance, a typical feature of covariance functions. Superimposed on the decay is an oscillation with a wavelength of approximately 2β, generated by the non-local predator–prey interaction. The reason for the oscillation is that a positive fluctuation at $x = 0$ gives more food, faster growth and a negative fluctuation near β, which in turn gives less food, slower growth and a positive fluctuation near 2β.

4 Discussion

We have presented a local stability analysis of the power-law steady state of marine size spectra. The approach has some resemblance to the local stability analyses of steady-state food webs widely applied in ecology (Murray 2002; Rooney et al. 2006). However, instead of having nodes representing a finite number of species, the analysis here uses a continuous weight range corresponding to an infinite number of "nodes", and this gives a continuous spectrum of eigenvalues. Characterization of the eigenvalue spectrum has been carried out before (Arino et al. 2004); the difference here is that we explicitly link growth of the organisms to predation, which we think is a useful step towards reality.

To do the analysis, the predator search exponent α and steady state exponent γ have been set so that $\alpha = \gamma - 1$. In addition, we assume that the rate for predation-independent death is independent of body weight. These assumptions imply that the dynamics of small perturbations are described by the convolution operator given in Eq. (12), leading to a simple time dependence of the perturbations in terms of an expansion in plane waves, given in Eq. (15). In general these assumptions would not be appropriate in ecological communities. The reason for using them here is that we believe it is valuable to have analytical results for this special case before beginning numerical explorations of conditions closer to those in nature.

The benchmark for the analysis is a jump-growth equation, obtained as the large-system limit of an underlying stochastic predation-growth process (Datta et al. 2010). Importantly, the eigenvalue spectrum of the well-known, first-order approximation, the McKendrick–von Foerster equation (Andersen and Beyer 2006; Law et al. 2009; Blanchard et al. 2009), exhibits a systematic departure from that of the jump-growth equation: the real parts of the eigenvalues of the former tend to zero as wavenumber increases, whereas those of the latter become increasingly negative. Therefore in our analysis the eigenvalue spectrum of the McKendrick–von Foerster equation must always contain eigenvalues with positive real parts, and must always have an unstable steady state.

In contrast to the first-order approximation, the eigenvalue spectrum of the second-order approximation, obtained by adding a diffusion term to the McKendrick–von Foerster equation, contains a negative term that is quadratic in the wavenumber, which makes the real parts of the eigenvalues much closer to those of the jump-growth equation. The diffusion term is potentially important. One consequence of it is that there can be eigenvalue spectra for which $\mathrm{Re}(\lambda(k)) < 0$ for all wavenumbers $k > 0$, implying local stability of the steady state. This is with the caveat that the eigenvalue spectrum tends to the natural death rate η as the wavenumber tends to zero, so perturbations with sufficiently low wavenumbers (long wavelengths) could still destabilize the steady state.

The second-order approximation with diffusion has not previously been used, but would be worth considering in the future when the full jump-growth equation cannot be used. Interestingly, Benoît and Rochet (2004) found they had to include a diffusion term in numerical integrations of the McKendrick–von Foerster equation to obtain a solution in the absence of natural mortality, although they stated that they did not understand why this should be so. How serious the omission of the diffusion term is

in practice depends on the wavenumber k at which the eigenvalue spectrum peaks, because it is this wavenumber that dominates the solution in the long term. If the peak occurs at sufficiently small k, the effect of the negative second-order term in Eq. (27) is small, and the standard McKendrick–von Foerster equation is reliable (Fig. 1). If the peak occurs at large k, the negative second-order term in Eq. (27) becomes significant, and inferences about stability from McKendrick–von Foerster equation may not be reliable (Fig. 2). The second-order equation with diffusion itself becomes a poor approximation if the feeding preference function is set such that predators are often smaller than their prey, because the Taylor expansion of the jump-growth equation on which it is based is no longer convergent (Datta et al. 2010). However, in reality predators are almost always larger than prey, so this is not likely to be an issue.

Key parameters for locating the peak of the eigenvalue spectrum with respect to k are the logarithm of the preferred predator:prey mass ratio β, the efficiency of mass transfer from prey to predator K and the diet breadth σ. The results in Sect. 3.5 suggest that predator–prey interactions would typically restrict the wavenumber k at the peak to be greater than π/β. Overall, to get the peak of the eigenvalue spectrum at a low wavenumber where the McKendrick–von Foerster equation works best, $Ke^{-\beta}$ must be small, i.e. growth increments of predators must be small. As β is made smaller and K is made larger, the McKendrick–von Foerster approximation works less well, because it misses the stabilizing effect of the diffusion term. The diet breadth σ, also affects the shape of the eigenvalue spectrum, the main effect in Eq. (27) being to dampen the oscillations in the real parts of the eigenvalues (Fig. 6). In so doing σ has the potential to shift positive peaks below $\mathrm{Re}(\lambda(k)) = 0$, and hence to change an unstable steady state into a stable one. This is consistent with the results of earlier studies which have shown the stabilizing effects of broad diets (Law et al. 2009; Datta et al. 2010).

Random variability from one individual to another in, for example, the number and size of prey items encountered over a period of time, can have important effects in systems such as the one studied in this paper. This intrinsic demographic stochasticity is distinct from environmental stochasticity, which is not included in the current model. Usually, the relative magnitude of fluctuations due to demographic stochasticity is proportional to $\Omega^{-1/2}$, where Ω is the total number of individuals in the system (van Kampen 1992). However, interaction between the natural frequency of the mean-field system and intrinsic variability, which acts at all frequencies, can cause resonant amplification of demographic stochasticity (McKane and Newman 2005). Stochastic effects can also cause switching between different solutions (see e.g. Samoilov et al. 2005), a phenomenon that cannot be investigated using the van Kampen (1992) approach taken in this paper, which deals with fluctuations about a mean-field solution. As seen in Fig. 7, correlations between simultaneous demographic fluctuations at different body sizes do exist. These arise from the predator–prey interactions described by the feeding kernel. An investigation of correlation of fluctuations across different times is beyond the scope of this paper. However, neither resonant amplification nor switching were observed in stochastic simulations, even for relatively small system size Ω, and the simultaneous correlations observed are likely to be very small for realistic system sizes.

A feature of the stability analysis here is that the parameter values required to achieve stability are outside the range likely to apply in marine systems (e.g. $K = 0.8$

in Fig. 2). As stated above, earlier numerical integrations using the McKendrick–von Foerster equation have led to stable steady states using realistic sets of parameter values. There are, however, some important differences between the present analysis and previous work. First, real size spectra span a finite range of body sizes, about twelve orders of magnitude being realistic (Cohen et al. 2003). This means that perturbations with very long wavelengths cannot occur, and corresponding to this, the wavenumber k cannot be less than about 0.2. Second, the finite range calls for lower and upper bounds which are not used here. Imposing such bounds removes the exact power-law steady state, and the boundary conditions themselves influence the stability of the steady state. Third, the constraint on parameter values needed to achieve $\alpha = \gamma - 1$ may exclude those values likely to lead to stability. The present study is best thought of as throwing light on the role that mortality, predation and growth play in determining stability of the power-law steady state. Other processes also leave their own footprint, and some of these increase the parameter space in which stable steady states arise (Capitan and Delius 2010).

Nonetheless, at a qualitative level, the results here are consistent with earlier observations that the steady state of marine size spectra undergoes a bifurcation from stability to instability as predator:prey mass ratio is increased and as diet breadth is decreased. The results here indicate that this is a Hopf bifurcation as a complex conjugate pair of eigenvalues cross the imaginary axis. Even without taking other major life processes into account, the analysis makes clearer what kinds of ecosystems are more vulnerable to external disturbances such as those caused by fishing and climate change. Further research should expand upon this, to better understand marine ecosystem dynamics, and better predict the potential consequences of perturbing seemingly robust ecosystems.

Acknowledgments The research was supported by a studentship to SD from the Natural Environment Research Council UK, with the Centre for Environment Fisheries and Aquaculture Science UK as the CASE partner. RL and MJP acknowledge support from the Royal Society of New Zealand Marsden fund, grant number 08-UOC-034. The research was facilitated by a Research Network Programme of the European Science Foundation on body size and ecosystem dynamics (SIZEMIC). We thank Julia Blanchard, Jennifer Burrow, Alex James, Jon Pitchford, Richard Rhodes, David Wall and the reviewers of the paper for their help and insights.

References

Andersen KH, Beyer JE (2006) Asymptotic size determines species abundance in the marine size spectrum. Am Nat 168:54–61

Anderson CNK, Hsieh C, Sandin SA, Hewitt R, Hollowed A, Beddington J, May RM, Sugihara G (2008) Why fishing magnifies fluctuations in fish abundance. Nature 452:835–839

Arino O, Shin Y, Mullon C (2004) A mathematical derivation of size spectra in fish populations. C R Biol 327(3):245–254

Aulbach B, Garay BM (1993) Linearizing the expanding part of noninvertible mappings. Z angew Math Phys 44(3):469–494

Benoît E, Rochet M (2004) A continuous model of biomass size spectra governed by predation and the effects of fishing on them. J Theor Biol 226(1):9–21

Blanchard JL, Jennings S, Law R, Castle MD, McCloghrie P, Rochet M, Benoît E (2009) How does abundance scale with body size in coupled size-structured food webs? J Anim Ecol 78(1):270–280

Boudreau P, Dickie L (1992) Biomass spectra of aquatic ecosystems in relation to fisheries yield. Can J Fish Aquat Sci 49(8):1528–1538
Camacho J, Solé RV (2001) Scaling in ecological size spectra. Europhys Lett 55(6):774–780
Capitan JA, Delius GW (2010) Scale-invariant model of marine population dynamics. Phys Rev E 81(6):061901
Cohen JE, Jonsson T, Carpenter SR (2003) Ecological community description using the food web, species abundance, and body size. Proc Natl Acad Sci USA 100(4):1781–1786
Datta S, Delius GW, Law R (2010) A Jump-Growth model for PredatorPrey dynamics: derivation and application to marine ecosystems. Bull Math Biol 72(6):1361–1382. http://arxiv.org/abs/0812.4968
Hsieh C, Reiss CS, Hunter JR, Beddington JR, May RM, Sugihara G (2006) Fishing elevates variability in the abundance of exploited species. Nature 443:859–862
Kirchgraber U, Palmer KJ (1990) Geometry in the neighborhood of invariant manifolds of maps and flows and linearization. Longman Scientific & Technical, Harlow
Law R, Plank MJ, James A, Blanchard JL (2009) Size-spectra dynamics from stochastic predation and growth of individuals. Ecology 90(3):802–811
McKane AJ, Newman TJ (2005) Predator–prey cycles from resonant amplification of demographic stochasticity. Phys Rev Lett 94:218102
Murray JD (2002) Mathematical biology, I: an introduction, 3rd edn. Springer, Berlin
Platt T, Denman K (1978) The structure of pelagic marine ecosystems. Rapports et Procés-Verbaux Des Réunions, Conseil International Pour l'Exploration de la Mer 173:60–65
Rooney N, McCann K, Gellner G, Moore JC (2006) Structural asymmetry and the stability of diverse food webs. Nature 442:265–269
Samoilov M, Plyasunov S, Arkin AP (2005) Stochastic amplification and signaling in enzymatic futile cycles through noise-induced bistability with oscillations. Proc Natl Acad Sci USA 102(7):2310–2315
Sheldon R, Parsons T (1967) A continuous size spectrum for particulate matter in the sea. J Fish Res Board Canada 24(5):909–915
Sheldon RW, Prakash A, Sutcliffe WH Jr (1972) The size distribution of particles in the ocean. Limnol Oceanogr 17(3):327–340
Silvert W (1980) Dynamic energy-flow model of the particle size distribution in pelagic ecosystems. In: Kerfoot W (ed) Evolution and ecology of zooplankton communities. University Press of New England, Hanover pp 754–763
Silvert W, Platt T (1978) Energy flux in the pelagic ecosystem: a time-dependent equation. Limnol Oceanogr 23(4):813–816
van Kampen NG (1992) Stochastic processes in physics and chemistry. Elsevier, Amsterdam
Ware DM (1978) Bioenergetics of pelagic fish: theoretical change in swimming speed and ration with body size. J Fisher Res Board Canada 35:220–228